Title
Acceleration of beam ions during major-radius compression in the tokamak fusion test reactor.

Journal
Physical review letters, 55(23)

ISSN
0031-9007

Authors
Wong, KL
Bitter, M
Hammett, GW
et al.

Publication Date
1985-12-01

DOI
10.1103/physrevlett.55.2587

Acceleration of Beam Ions during Major-Radius Compression in the Tokamak Fusion Test Reactor

K. L. Wong, M. Bitter, G. W. Hammett, W. Heidbrink, H. Hendel,[a] R. Kaita, S. Scott, J. D. Strachan, G. Tait, M. G. Bell, R. Budny, C. Bush,[b] A. Chan, J. Coonrod, P. C. Efthimion, A. C. England,[b] H. P. Eubank, E. Fredrickson, H. P. Furth, R. J. Goldston, B. Grek, L. Grisham, R. J. Hawryluk, K. W. Hill, D. Johnson, J. Kamperschroer, H. Kugel, C. Ma,[b] D. Mansfield, D. Manos, D. C. McCune, K. McGuire, S. S. Medley, D. Mueller, E. Nieschmidt,[c] D. K. Owens, V. K. Paré,[b] H. Park, A. Ramsey, D. Rasmussen,[b] A. L. Roquemore, J. Schivell, S. Sesnic, G. Taylor, M. D. Williams, and M. C. Zarnstorff

Princeton Plasma Physics Laboratory, Princeton University, Princeton, New Jersey 08544

(Received 26 July 1985)

Tangentially coinjected deuterium beam ions were accelerated from 82 up to 150 keV during a major-radius compression experiment in the tokamak fusion test reactor. The ion energy spectra and the variation in fusion yield were in good agreement with Fokker-Planck code simulations. In addition, the plasma rotation velocity was observed to rise during compression.

PACS numbers: 52.50.Lp, 52.40.Mj, 52.50.Gj, 52.55.Fa

The tokamak fusion test reactor (TFTR) project was initiated to study tokamak physics near D-T break-even conditions ($Q = P_{\text{fusion}}/P_{\text{heat}} \simeq 1$) in a two-component plasma,[1] because the $n_e\tau_E$ requirement for break-even was considerably less stringent than the conventional Lawson criterion. The practical implementation of the two-component approach is through neutral-beam injection.[2] If W_0 denotes the injection energy of the deuterium beam, the optimum Q near break-even is expected to occur at $W_0 \simeq 150$–300 keV. It was pointed out by Furth and Jassby[3] that substantial improvement in Q can be achieved by clamping the injected ions at the energy giving the maximal ratio of fusion-reaction rate to plasma drag, rather than injecting at higher energy and passing through the optimal region during deceleration. One proposed method was to inject tangential beams, accelerate the beam ions to the optimal energy by rapid magnetic compression in major radius,[4,5] and then maintain this energy by slow compression. Compressional acceleration of low-energy beam ions (~ 15 keV) was first observed in the Princeton adiabatic toroidal compressor (ATC).[5] In this Letter, we present experimental results which demonstrate that magnetic compression in major radius can accelerate tangentially injected beam ions from 82 keV up to 150 keV, accompanied by enhanced fusion neutron emission. The evolution of the fast-ion energy-distribution function during compression was investigated in detail for the first time and good agreement was found between the experiment and a Fokker-Planck simulation. Unlike the ATC experiment,[5] plasma rotation was also observed, and its change during compression was roughly consistent with conservation of angular momentum.

The experiment was performed in TFTR with the following plasma parameters before compression: plasma major radius $R = 3.0$ m, minor radius $a = 0.57$ m, plasma current $I_p = 450$ kA, toroidal magnetic field $B_0 = 3.3$ T at $R = 3.0$ m, central electron temperature $T_e(0) \sim 3.3$ keV, central deuterium-ion temperature $T_i(0) \sim 3.8$ keV, and central and line-averaged electron densities 1.7×10^{13} cm^{-3} and 1.3×10^{13} cm^{-3}, respectively. 82-keV deuterium neutral beams at 2.1 MW were injected parallel to the toroidal plasma current from $t = 2.3$ to 2.5 sec. At $t = 2.5$ sec, the plasma major radius was compressed to 2.17 m by the raising of the vertical magnetic field. Figure 1 shows the waveforms of I_p, n_eL, and R in a typical plasma shot. Data from the multichannel Thomson-scattering system and the electron-cyclotron-emission diagnostic were used to determine the evolution of R, $n_e(r)$, and $T_e(r)$ during compression. A five-chord infrared interferometer was also used to determine the plasma-density profile. The locations of maximum electron density were obtained by a standard five-point spline-fitting technique, and they are compared with multichannel Thompson-scattering results in Fig. 1(b). The agreement is reasonably good throughout the compression duration of approximately 15 ms. The post-compression $T_e(0)$ and $n_e(0)$ were somewhat lower than expected from adiabatic scaling. This feature has been described in some detail previously,[6] and is outside the scope of this Letter.

Two charge-exchange neutral-particle analyzers were used to measure the ion-energy spectra before and after compression. One analyzer was aimed approximately along the post-compression magnetic axis, while the second analyzer was aimed for tangency at $R = 0.52$ m. The change in the ion-energy spectra due to compression is depicted in Fig. 2. The charge-exchange spectra were averaged over 10 ms, and all

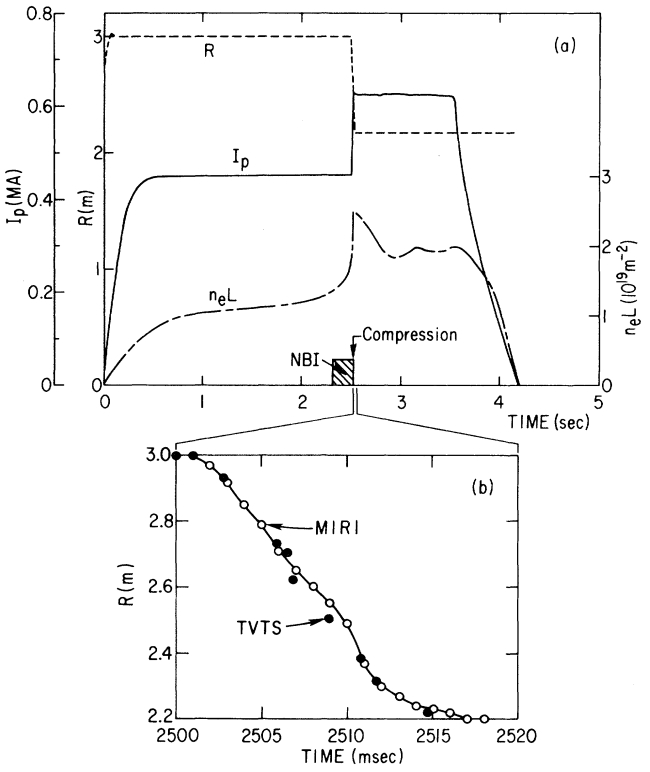

FIG. 1. (a) Experimental wave forms for plasma current, line-integrated density, and plasma major radius. (b) Plasma major radius on expanded time scale, the dots being Thomson-scattering data (TVTS) and the open circles being results from the five-chord infrared interferometer (MIRI). Compression starts at 2.5 sec.

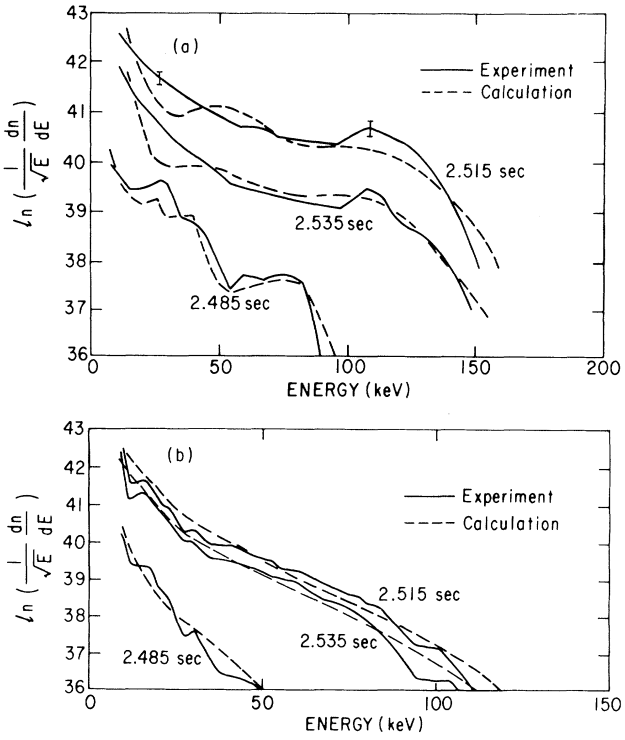

FIG. 2. Comparison of charge-exchange spectra with simulation by Fokker-Planck code (dashed lines). The error bars of ± 0.13 e-folds represent the uncertainty introduced by anode-to-anode efficiency-gain variations. (a) Charge-exchange analyzer viewing approximately tangential to the toroidal field at $R = 2.19$ m. (b) Charge-exchange analyzer viewing at $R = 0.52$ m.

the spectra shown in this figure were taken during the same shot. Before compression, the ion-energy-distribution function showed a cutoff near the injection energy (82 keV). This cutoff energy was raised to 150 keV immediately after compression. This was expected for the compression ratio $C = 1.38$, since the energy of particles moving along magnetic field lines increases by a factor of C^2. In order to interpret these data quantitatively, a bounce-averaged Fokker-Planck code[7,8] was used to follow the ion-distribution function $f(E,\xi,r,t)$ in time as a function of energy, pitch angle, and minor radius. Since the equipartition time for the beam ions is much longer than the compression time (~ 15 ms), we can treat the beam-ion angular momentum about the major axis, $v_\phi R \simeq v_\parallel R$, and the magnetic moment $\mu = \frac{1}{2} m v_\perp^2 / B$, as invariant quantities. This means that $dv_\parallel/dt \simeq -(v_\parallel/R)(dR/dt)$ and $dv_\perp/dt \simeq -(v_\perp/2R)(dR/dt)$. Utilizing these results together with the usual effects of classical collisional slowing down, energy diffusion, pitch-angle scattering, neutral-beam injection, and charge-exchange losses, we solve for f, and the charge-exchange spectra can then be calculated along different sight lines at various times. The results are shown by the dashed lines in Fig. 2. Interpretation of the neutral spectra is complicated by the fact that it is a sight-line-integrated measurement over the plasma. Discrepancies between theory and measurement of the magnitude observed in Fig. 2 have been observed in other experiments.[8] Uncertainties in the toroidal and radial dependence of the neutral-density profile, in particular, can give rise to errors of a factor of 2 in the simulation of charge-exchange spectra. In addition, the features at 110 keV in the post-compression experimental spectra are due to variations in the instrument gains.

For the modeling of charge-exchange losses, the neutral density was calculated with use of a one-dimensional radial code, and normalized to give a global particle-confinement time of 170 ms. This is approximately a factor 2 larger than the particle-confinement time estimated for the precompression phase, in part to correct for the recapture of escaping fast ions being ignored. With this assumption, collisional drag dominates over charge-exchange losses by a factor 3.5 for beam ions at the center of the plasma,

or 1.5 when averaged over the whole plasma. Since reasonable agreement with the data is obtained, however, for a conservatively low value of the neutral density, there does not seem to be any anomalous loss of fast ions during compression. This is also consistent with a central-particle-confinement time that is much longer than the compression time. Since the neutral-density variation during compression is not known, we cannot calculate the absolute magnitude of the charge-exchange signal. After compression, $dR/dt = 0$, and the decay of the fast ion energy is observed to behave classically.

The fusion neutron yield was observed to increase by a factor 5.2 ± 0.8 during compression, with the uncertainty being due to the dependence of detector sensitivity on the plasma major radius. In this experiment, the neutron emission comes mainly from beam-target interactions. If all of the reactions were due to parallel 80-keV beam ions, the emission should increase by a factor 1.9 as a result of the density rise and an additional factor 3.3 in reactivity as the beam ions accelerate up the $d(d,n)^3$He cross sections. Coulomb drag and energy diffusion of the beam reduce the expected increase below this ideal value. The measured neutron yield is compared with that calculated from the Fokker-Planck code in Fig. 3(a). The dashed line represents the calculated neutron yield rescaled to fit the experimental data, which is about half of the value expected if the $Z = 1$ plasma ions are assumed to be 100% deuterium. With consideration of the uncertainties in the neutron detector calibration, deuterium concentration, neutral-beam species mix, and deposition profile, a factor 2 discrepancy in absolute magnitude is within experimental error.[9] With these caveats, the neutron yield simulation suggests that the absolute magnitude, as well as the shape, of the energetic ion-distribution function is not far from the Fokker-Planck code simulation. With 4 MW of neutral-beam power, a peak neutron yield of 6×10^{14}/sec was observed, which is the highest so far achieved in TFTR.

The $d(d,n)^3$He cross section increases by a factor 2.3 when the deuteron energy goes from 80 to 150 keV. A more sensitive indication of deuteron energy is provided by the ^{3}He$(d,p)\alpha$ reaction for which the cross section increases 10 times over the same energy range. A small amount of ^{3}He gas was puffed into the vacuum vessel 250 ms before compression (at $t = 2.25$ sec), just before injection of the 82-keV D^0 beams. The 15-MeV protons produced by d-^{3}He reactions were unconfined in this experiment, and were detected by surface-barrier detectors situated at the bottom of the vacuum vessel. Figure 3(b) shows that the proton-detector signal was increased over an order of magnitude by the compression. It should be noted that the proton-detector efficiency has considerable

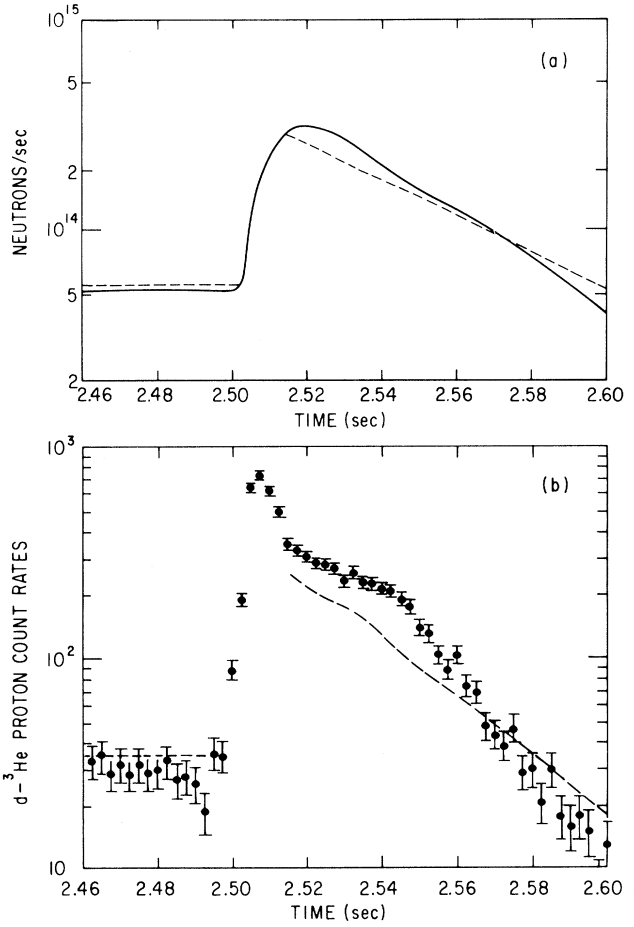

FIG. 3. Fusion-product measurements. (a) Neutron yield from $d(d,n)^3$He reaction. The statistical error is negligible, and the relative error between precompression and post-compression plasma due to calibration uncertainties is $\pm 15\%$. (b) Proton-count rate from ^{3}He$(d,p)\alpha$ reaction. The error bars only represent statistical errors. The dashed lines indicate the Fokker-Planck code simulations, including the detector efficiency.

uncertainty and varies during compression because the 15-MeV proton orbits which reach the detector depend upon the plasma position. Orbit-code calculations[10] indicate that the efficiency for the post-compression plasma is about $0.5^{+0.5}_{-0.25}$ times the value for the precompression plasma. Thus the d-^{3}He reaction rate increased by about 25 times after the beam ions were accelerated. The error bars shown in Fig. 3(b) represent only the statistical error. The major experimental uncertainty is due to the dependence of detector sensitivity on plasma major radius, and the discrepancy between measurement and simulation results is within this uncertainty.

Following compression, both the d-d and the d-^{3}He emission decay because of Coulomb relaxation of the

beam ions. Our main interest is in the change of reaction rate during compression. In the Fokker-Planck simulation we have used electron temperature and density profiles that are constant in time after compression, while in the experiment there were small variations in these parameters, sufficient to account for the small discrepancies in the emission decay rates after compression. Detailed comparison of these results will be published separately.

The coinjecting neutral beams in this experiment caused the toroidal plasma to rotate about its major axis.[11] Compression began after the rotation speed reached a steady value, i.e., when the torque delivered by the beam particles was balanced by damping. Because of the finite slowing-down time of the beam particles, this balance was approximately maintained during compression, so that the plasma angular momentum was nearly conserved. The central rotation velocity $v_\phi(0)$ was thus expected to increase approximately by the compression ratio $[v_\phi(0) \rightarrow C v_\phi(0)]$, provided that the radial profile $v_\phi(r)$ remained unchanged. In the experiment, $v_\phi(0)$ was measured by the Doppler shift of the Ti XXI $K\alpha$ line which was emitted mainly from the center of the plasma.[12] Figure 4 shows the variation of $v_\phi(0)$ with time for a typical compression shot. The vertical and horizontal bars indicate the statistical error and the time resolution of the data points. The change of $v_\phi(0)$ during compression is represented by the two data points taken with a time resolution of 10 ms in the time interval from 2.500 to 2.520 sec. $v_\phi(0)$ increased by a factor 1.28, which is somewhat smaller than the compression ratio ($C = 1.38$). Unfortunately, mechanical vibrations of 35 Hz began to affect the signal at $t > 2.530$ sec, and caused the signal to oscillate between the limits shown by the dashed curves in Fig. 4 when fast time resolution was employed. Interferences from these 35-Hz mechanical vibrations were also observed by other diagnostics, e.g., by the infrared interferometer. The data points used to determine the change of $v_\phi(0)$ due to compression were not affected by vibration. After the onset of the mechanical vibration, 80-ms time bins were used to average out the oscillations. From the exponential decay of these data points we deduce an angular-momentum-confinement time of 0.3 sec for the post-compression plasma. This value is comparable to those obtained in noncompression shots where interferences from mechanical vibration were not present. Detailed analysis of these data, including the effects of finite momentum-confinement time, beam slowing down, and sawtooth activity will be given in a separate paper.

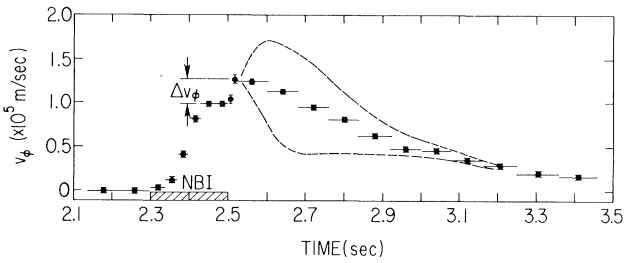

FIG. 4. Central toroidal-plasma-rotation velocity vs time from Doppler-shift measurement of the Ti XXI $K\alpha$ line. The dashed lines bracket the signal oscillations (caused by mechanical vibrations) which are eliminated by averaging over 80-ms intervals.

We are grateful to the many engineers, computer programmers, technicians, and other staff members who have supported the TFTR program. Special thanks are due to Professor T. H. Stix for his critical reading of the manuscript. This work was supported by U.S. Department of Energy under Contract No. DE-AC02-76-CHO-3073.

[a]Permanent address: RCA David Sarnoff Research Center, Princeton, N.J. 08450.

[b]Permanent address: Oak Ridge National Laboratory, Oak Ridge, Tenn. 37830.

[c]Permanent address: Idaho National Engineering Laboratory, EG&G Idaho, Inc., Idaho Falls, Ida. 83415.

[1]J. M. Dawson, H. P. Furth, and F. H. Tenney, Phys. Rev. Lett. **26**, 1156 (1971).

[2]H. Eubank *et al.*, Phys. Rev. Lett. **43**, 270 (1979).

[3]H. P. Furth and D. L. Jassby, Phys. Rev. Lett. **32**, 1176 (1974).

[4]H. P. Furth and S. Yoshikawa, Phys. Fluids **10**, 2593 (1970).

[5]K. Bol *et al.*, Phys. Rev. Lett. **32**, 661 (1974).

[6]G. Tait *et al.*, in *Proceedings of the Tenth International Conference on Plasma Physics and Controlled Nuclear Fusion Research, London, 12–19 September 1984* (International Atomic Energy Agency, Vienna, 1985), Vol. I, p. 141.

[7]J. G. Cordey, Nucl. Fusion **16**, 499 (1976); see also R. Goldston, Ph.D. thesis, Princeton University (1977).

[8]R. Kaita *et al.*, Nucl. Fusion **25**, 939 (1985).

[9]J. D. Strachan *et al.*, Nucl. Fusion **21**, 67 (1981).

[10]W. W. Heidbrink and J. D. Strachan, Rev. Sci. Instrum. **56**, 501 (1985).

[11]R. C. Isler *et al.*, Phys. Rev. Lett. **47**, 649 (1981).

[12]M. Bitter *et al.*, Phys. Rev. A **32**, 3011 (1985).